Published in final edited form as:
J Bone Miner Res. 2012 May ; 27(5): 1018–1029. doi:10.1002/jbmr.1567.

Demonstration of Osteocytic Perilacunar/Canalicular Remodeling in Mice during Lactation

Hai Qing[1,*], **Laleh Ardeshirpour**[2,*], **Paola Divieti Pajevic**[3], **Vladimir Dusevich**[1], **Katharina Jähn**[1], **Shigeaki Kato**[4], **John Wysolmerski**[5], and **Lynda F. Bonewald**[1,6]

[1]School of Dentistry, University of Missouri-Kansas City, Kansas City, MO, 64108, USA

[2]Section of Pediatric Endocrinology, Department of Pediatrics, Yale University School of Medicine, New Haven, CT, 06520, USA

[3]Endocrine Unit, Massachusetts General Hospital, Harvard Medical School Boston, MA 02114, USA

[4]Institute of Molecular and Cellular Biosciences, University of Tokyo, Tokyo, Japan

[5]Section of Endocrinology and Metabolism, Department of Internal Medicine, Yale University School of Medicine, New Haven, CT, 06520, USA

Abstract

Osteoclasts are thought to be solely responsible for the removal of bone matrix. However, we show here that osteocytes can also remove bone matrix by reversibly remodeling their perilacunar/canalicular matrix during the reproductive cycle. In contrast, no osteocytic remodeling was observed with experimental unloading despite similar degrees of bone loss. Gene array analysis of osteocytes from lactating animals revealed an elevation of genes known to be utilized by osteoclasts to remove bone including Tartrate Resistant Acid Phosphatase, *TRAP*, and *cathepsin K* that returned to virgin levels upon weaning. Infusion of Parathyroid Hormone Related Peptide, PTHrP, known to be elevated during lactation, induced TRAP activity and cathepsin K expression in osteocytes concurrent with osteocytic remodeling. Conversely, animals lacking the Parathyroid Hormone Type 1 receptor, PTHR1, in osteocytes failed to express TRAP or cathepsin K or to remodel their osteocyte perilacunar matrix during lactation. These studies show that osteocytes remove mineralized matrix through molecular mechanisms similar to those utilized by osteoclasts.

Introduction

Recently, it has been recognized that osteocytes, the most abundant cells in bone, play a significant role in bone health and disease[(1)]. These cells are multifunctional as emphasized by their capacity to orchestrate skeletal remodeling by regulating osteoblasts[(2)] and osteoclasts on the bone surface[(3)], to regulate phosphate homeostasis[(4)] and to mediate the effects of mechanical forces on the skeleton[(3)]. However, it has remained controversial whether osteocytes play an active role in calcium homeostasis and whether this cell can remodel its bone microenvironment[(5–7)]. The osteocyte lacuno-canalicular network provides access to an extremely large internal bone surface and it has been estimated that removal of only a few angstroms of mineral per osteocyte would have significant effects on circulating ion levels[(8)].

[6]Corresponding author: L.F. Bonewald, Ph.D., Tel: 816 235-2068, Fax: 816 235-5524, bonewaldl@umkc.edu.
[*]contributed equally to this work.

The authors have no conflict of interest.

The skeleton is an important source of calcium during lactation. In humans, lactation is associated with a 5–8% decline in bone mineral density (BMD) over 6 months, a rate of bone loss approximately 10-times faster than that occurring after menopause. Lactating mice lose 20–30% of bone mineral over the course of lactation[9, 10]. However, previous data demonstrated that inactivation of osteoclasts with pamidronate treatment only blocked the decline in BMD during lactation by 60%, suggesting additional mechanisms of bone mobilization other than osteoclasts during this period[11, 12]. Based on these observations, we hypothesized that, in addition to osteoclasts, osteocytes might also play a role in mobilizing bone mineral during lactation.

Methods

Animal experiments

Twelve-week-old, CD1 mice purchased from Charles River Laboratories (Wilmington, MA) were allowed to become pregnant, deliver and lactate as described previously[11]. Litter size was adjusted to 8–13 pups to equalize suckling intensity between dams. Pups were removed on the 12th day of lactation to induce weaning and skeletal recovery. Age-matched, virgin CD1 mice were used as controls. Mice were sacrificed on the 12th day of lactation or the 7th day after forced weaning. Age-matched, virgin CD1 mice were used as controls.

In order to study a mechanical-disuse bone loss, 14 CD1 female mice the same age as in the lactation experiments were randomly divided into 2 groups. The mice in the unloaded group were tail-suspended to unload the hind limbs for 4 weeks. To control for stress, control mice were also tail-attached with the same suspension device, but without unloading of the hind limbs. Body weight was measured before tail-suspension and again before sacrifice.

PTHrP-treated mice received a continuous infusion of PTHrP (1–36) subcutaneously using Alzet mini-osmotic pumps (model 2002) at a rate of 10pmol/hr until sacrifice on day 12, as described in our previous publications[13].

Mice lacking the PTHR1 in osteocytes (PTHR1-cKO) were generated by crossing 10KbDMP1-Cre mice expressing promoter activity in some bone surface cells, newly embedding osteocytes, and embedded osteocytes[14] with mice in which exon1 of the PTHR1 was flanked by Lox-P sites[15]. Successful ablation of the PTHR1 from osteocyte was assessed by real-time quantitative polymerase chain reaction (qPCR) using primers specific for the floxed allele. After validation with PCR, 12-week-old PTHR1-cKO mice as well as control littermates were subjected to the lactation conditions as mentioned above.

Ctsk-Cre/R26R mice were generated by crossing R26R mice[16] with Ctsk-Cre mice[17]. Twelve to 14 week old virgin and age-matched, lactating Ctsk/R26R mice were studied at day 12 of lactation and were compared to age-matched, control female R26R virgin and lactating mice.

All mice were housed in standard conditions of temperature (23 ± 2°C) and light-controlled environment (12-h light/12-h dark cycle), and had free access to water and pelleted food (UAR rodent diet No. R03-25; UAR, Epinay/Orge). All animal experiments were approved by the University of Missouri at Kansas City, the Institutional Animal Care and Use Committee of Massachusetts General Hospital or the Yale University IACUC committees in accordance with regulations and guidelines.

Dual-energy x-ray absorptiometry

BMD of left proximal tibia was measured by DEXA in all animals before sacrifice using a Lunar densitometer PIXImus (G.E. Medical Systems, Lunar Division, Madison, WI;

software version 1.45). Mice were anesthetized with 50 mg/kg ketamine (Ketaset III; Fort Dodge Animal Health, Fort Dodge, IA) and 10 mg/kg xylazine (AnaSed; Lloyd, Shenandoah, IA) by ip injection before analysis.

Micro-computed tomography

DEXA data were further confirmed using μCT. Tibiae were dissected and fixed in 10% neutralized formalin for 2 days, and then analyzed using x-ray μCT (vivaCT40; Scanco Medical AG, Bassersdorf, Switzerland). Specimens were scanned at 55 kV (145 A), using 1000 cone beam projections per revolution and an integration time of 300 ms within a 12.3-mm-diameter field of view. Three-dimensional images within the range of 0 to 1.2 mm from the most proximal metaphysis of tibiae were reconstructed. Bone morphometry was characterized with bone volume fraction value and BMD. Trabecular morphometry from the same region was further studied by excluding the cortical bone from the endocortical borders, and was characterized with bone volume fraction (BV/TV), BMD, trabecular thickness (TB.TH), trabecular number (TB.N), trabecular spacing (TB.Sp), and connectivity density.

Backscatter scanning electron microscopy (BSEM) for quantitation of lacunar area

Freshly dissected tibiae, lumbar vertebrae and calvarial bones were stripped of soft tissue, and placed in 20 ml of 10% neutral phosphate buffered formalin, After fixation, samples were washed with PBS, transferred to 70% ethanol for 4–24 h. All of the bones were dehydrated in graded ethanol (95%, two baths; 100%, four baths), for at least 4 hours each at 4°C. Following dehydration, they were placed in infiltration medium containing 85% destabilized methyl methacrylate (MMA; Sigma, St. Louis, MO), 15% dibutyl phthalate (Sigma), and 0.15% benzoyl peroxide (Polysciences, Inc., Warrington, PA). After three days under vacuum, the bones were removed from the infiltration MMA and placed on pre-polymerized base layers, covered with freshly catalyzed MMA, and incubated for two days at 37.8ºC in a radiant heat oven (Labline, Melrose Park, IL). Glass vials were removed from the oven, cooled at −20.8°C for 1 h, and the specimen blocks removed by breaking the glass. Specimen blocks were trimmed, sectioned, and sequentially polished. The BSEM was used to image the osteocyte lacunae on the sectioned bone surface in the standardized areas. With the analysis software, the images were thresholded. Then the areas of approximately 250 lacunae from each sample were measured in a blinded fashion.

SEM of acid-etched resin embedded sections

To further validate the results from backscatter SEM, the same samples were acid etched with 37% phosphoric acid for 12 seconds, then washed with distilled water and commercial bleach as described previously[4]. SEM was used to image completely exposed resin-casted lacunae, and lacunar area was measured using the Analysis software. Approximately 4–5 lacunae per treatment group were randomly selected and 6–10 canaliculi were quantified per lacunae. The diameter of the canaliculi was determined by selecting canaliculi where the diameter did not vary for 0.5 μm from the surface of the lacunar resin caste.

Double fluorochrome labeling

To label the mineral being replaced within lacunae on the perilacunar matrix, calcein green (5 mg/kg i.p) and Alizarin red (20 mg/kg i.p) were injected into the mice at different time points. For the post-lactation group, mice were injected with calcein green on the first day after weaning, followed by Alizarin red on the 4th day, and were sacrificed on the 7th day. Lactating mice were injected with calcein green 2 days before delivering, then with Alizarin red on the 10th day after delivery and were sacrificed on the 12th day. Virgin mice were treated at the same time points as the lactation group. After sacrifice, tibiae were dissected

and embedded in MMA as described above. 10-μm thick sections were inspected using fluorescent microscopy (Nikon Eclipse E800).

Tartrate resistant acid phosphatase staining

Paraffin sections (5 μm) from right femurs were dewaxed, rehydrated, and stained for tartrate resistant acid phosphatase activity using the standard naphthol AS-BI phosphate post coupling method with some minor modification. The slides were incubated for 45 min at 37ºC in 0.92% sodium acetate buffer, pH 5.0, containing 0.01% naphthol AS-BI phosphate and 1.14% L-(+)Tartaric acid. Then, the sections were incubated in the same buffer containing 0.1% pararosaniline chloride for 10 min, followed by washing in distilled water. The sections were counterstained with hematoxylin for 4 minutes, dehydrated and coversliped with permount. TRAP-positive osteocytes within 8 mm to 9 mm from the proximal end of the femur were quantified in a blinded fashion.

Microarray analysis

Tibiae from virgin, lactating, and post-lactation mice (n=3 different mice in each group yielding 9 gene arrays) were processed immediately after sacrifice. Osteocyte RNA was extracted from tibia diaphyses after sequential digestion to remove surface cells such as osteoclasts and osteoblasts. As previously described[18], soft tissue and periosteum were removed from the femurs, the epiphyses were cut off and bone marrow was removed by centrifugation. Diaphyses were submitted to three sequential incubations at 37°C with 0.2% type 1 collagenase (Sigma)/ 0.05% trypsin (Sigma) for 30 minutes, and then were washed with PBS. Then the bones were digested in 0.53 mM EDTA/ 0.05% trypsin (Cellgro, Mediatech, Inc, Manassas, VA) at 37°C for 30 min, rinsed with PBS and digested with 0.2% collagenase/ 0.05% trypsin solution at 37°C for 30 min. Finally, the diaphyses were rinsed with PBS, pulverized in liquid nitrogen, and the resulting bone powder added to Trizol reagent (Invitrogen, Carlsbad, CA). Total RNA was isolated as per the Trizol manufacturer's instructions. The gene expression profile of the osteocytes was determined using the Affymetrix GeneChip system Mouse 430 2.0 array (Affymetrix, Santa Clara, CA). Sample amplification, labeling, hybridization and scanning were carried out by the microarray core of the Kansas University Medical Center, Kansas City, KS. Briefly, 100 ng total RNA was reversely transcribed to cDNA, subjected to T7 mediated *in vitro*-transcription amplification and labeling followed by hybridization to the array for 16 hours at 45°C. The array was washed and stained with streptavidin-phycoerythrin on the GeneChip® Fluidics Station 450, and scanned using the GeneChip® Scanner 3000 7G with autoloader. The RMA algorithm was applied to the raw data to generate intensity values. Gene filtering was then applied to identify significantly differentially regulated genes. Filters included: background filter and fold change filter (1.5 fold). Gene lists were analyzed using Bioconductor with one-way ANOVA Analysis. The data sets can be found under: http://www.ncbi.nlm.nih.gov/geo/query/acc.cgi?acc=GSE23496.

Quantitative real-time-polymerase chain reaction

To validate the microarray data, the same RNA extraction procedure was used to extract osteocyte RNA. cDNA were synthesized using the High Capacity cDNA reverse transcription kit. Real-time qPCR was carried out in an ABI7000 sequence detector (Applied Biosystems, Foster City, CA) using Pre-made Gene Expression Assays (Applied Biosystems) primers and probes for *ACP5* (TRAP) and *Ctsk*. Levels of mRNA were calculated based on the CT values and normalized by *mouse GAPDH* expression.

Immunohistochemistry

Immunohistochemistry using a polyclonal Rabbit antibody (ABcam ab19027) was used to visualize cathepsin K expression in osteocytes. Freshly dissected femurs were fixed in 4% paraformaldehyde in PBS at 4ºC for 2 h and were then decalcified in a 10% EDTA solution in PBS at 4ºC for 3 weeks. Samples were washed in PBS and sequentially dehydrated and embedded in paraffin. Paraffin sections (5 μm) were stained with the primary antibody against cathepsin K (1:75) for 4 hours at room temperature. Detection of the primary antibody was performed using a peroxidase-conjugated secondary goat anti-rabbit IgG antibody (1:200 Immuno research) and DAB. Non-immune rabbit IgG served as a negative control. The cathepsin K staining was evaluated by a person blinded to the identity of the sample and was scored as positive cells

Analysis of LacZ expression in Ctsk-Cre/R26R bones

Ctsk/R26R and control R26R tibia were freshly dissected and fixed in 2% paraformaldehyde with 0.02% glutaraldehyde buffered in PBS for 1 hour on ice. After washing with PBS, the bones were stained with X-gal solution (0.1% 4-chloro-5-bromo-3-indolyl-D-galactopyranoside, 2 mM MgCl2, 5 mM EGTA, 0.02% Nonidet P-40, 5 mM K3Fe(CN)6, and 5 mM K4Fe(CN)6·3 H2O) at 30°C overnight. Bones were decalcified in 4% EDTA at pH 7.4 for 2 weeks. Samples were washed in water, dehydrated and embedded in paraffin as described previously[19].

Statistical analysis

Values are expressed as mean±SD, and error bars represent SD. A p value of 0.05 or less was used as the criteria for statistical significance. When comparing three or more groups, one-way ANOVA followed with the Newman-keuls post-test was used for parametric test. For non-parametric test, the Kruskal-wallis test was used. To compare two groups, the unpaired, two-tailed Student's t test was used. All statistical analyses were performed using GraphPad InState 3.06 for Windows (GraphPad Software, San Diego, CA).

Results

Osteocyte lacunar area is reversibly increased during lactation

Several bones were screened by BSEM to determine if significant differences could be observed in osteocyte lacunar size between virgin and lactating animals. Tibia, femur, vertebra, and calvaria cortical bones were compared. Consistent significant increases in lacunar size were observed in tibiae from lactating animals whether the top 20% of the largest lacunae were used as described previously[20] or even if 100% of lacunae were compared (Figure 1). Similar increases in lacunar size with lactation as those found with tibiae were also found in lumbar vertebrae (Figure 1) and femori (data not shown), but not in calvariae (Figure 1). Osteocyte lacunar area, μm^2, was significantly increased in cortical vertebral bone during lactation whether the 20% of the largest were compared (91.1±13.9* lactation, 64.0±7.4 virgin mice $p< 0.05$) or whether 100% of all lacunae were compared; (32.1±4.0*) as compared to virgin (24.6±5.1). No significant changes were observed in osteocyte lacunar area in calvaria. Therefore, the tibia was chosen for quantitation of lacunar area followed by the vertebrae for the following experiments.

To ensure that bone loss was occurring in the tibia as has been shown previously in the spine and femur with lactation[11, 21], PIXImus analysis of the left proximal tibiae was performed and showed a significant reduction in the BMD of lactating mice as compared to virgin controls (lactating: 0.065±0.002, vs. control: 0.077±0.001 mg/cm^2, 18.3% loss in BMD $p<0.01$). Seven days after forced weaning, BMD had increased (0.067±0.001, 3.1% increase, $p<0.05$), but was still significantly lower than the virgin controls. Next, we used

BSEM to examine osteocyte lacunar area in both cortical and trabecular tibial bone during the rapid bone loss of lactation and during the rapid recovery period following weaning. We found that lacunar area increased significantly in both tibial cortical bone (Figure. 2a,b) and tibial trabecular bone (Figure. 2c) during lactation (44.85±3.93* μm^2 cortical; 46.74±6.53* μm^2 trabecular) as compared to virgin controls (37.77±2.19 μm^2 cortical; 38.24±5.34 μm^2 trabecular $p>0.05$). Seven days after weaning, when bone mass was rapidly increasing, the tibial osteocyte lacunar area decreased (37.78±3.43 μm^2 cortical; 36.99±3.84 μm^2 trabecular) and was similar to that of virgin mice.

The BSEM results were validated by quantification of resin-casted lacunae, which showed a similar increase in osteocyte lacunar area with lactation and a subsequent decrease post-lactation (Figure 2d,e,f). To determine, if mineral was removed from around the osteocyte dendritic processes, which have even larger internal bone surface than lacunae[22], the same resin-casted scanning electron microscopy[23] images were used to measure canalicular diameter. An increase in canalicular diameter was observed in cortical bone from lactating animals (virgin 0.26±0.04 μm, lactating 0.31±0.04 μm, $p=0.054$) and a significant increase in canalicular diameter was observed in trabecular bone (virgin 0.24±0.03 μm, lactating 0.36±0.02 μm) (Figure 2g).

The return of the osteocyte lacunar area to virgin levels one week after forced weaning suggested that new mineral might be deposited by the osteocytes within lacunae during this time. To determine if this was the case, animals were injected with two different fluorochromes four days apart and tibiae were examined using fluorescence microscopy. As shown in Figure 2h, two distinctive lines of fluorochrome labeling, calcein green (first injection) and Alizarin red (second injection) (small insert), can be found at the bone surface of the virgin and post-lactation animals with only an intermittent, single green line in the lactating animal (small insert). Interestingly, in the virgin animals, some label was taken up by the newly embedded osteocytes close to the mineralization front at the periosteal surface; however the intensity was considerably less than labeling of the bone surface. In the lactating animals, only lacunae with the single faint green label were observed. In the post-lactation animals, both fluorochromes could be seen labeling osteocyte lacunae located well away from the bone surfaces (arrows), suggesting perilacunar mineral deposition by osteocytes.

Unloading does not increase osteocyte lacunar area

To determine if the changes in osteocyte lacunae were simply a function of rapid bone loss, we also studied the hind-limb suspension model of skeletal unloading, which like lactation, also leads to rapid bone loss. As shown in Figure 3, we found no significant differences in cortical osteocyte lacunar area (29.47±1.84 μm^2) compared to controls (29.30±1.95 μm^2) in the tibiae of hind-limb-unloaded mice (Figure 3a,b). To ensure that BMD had significantly decreased with unloading, both DEXA and μCT was performed. BMD significantly decreased ($p<0.0001$, 7.4% bone loss) in the left femur of unloaded mice (0.068±0.001* mg/cm^2) as compared to controls (0.073±0.001). The loss in BMD in unloaded mice was further confirmed by μCT (Figure 3d) of both cortical and trabecular bone in the proximal tibiae. Similar to the DEXA results, μCT analysis showed that cortical and trabecular BMD/TV and bone volume fraction (BV/TV) of the proximal tibiae in the unloaded group were significantly decreased compared to controls (Figure 3 c, table e). Likewise, the unloaded groups showed a significant decrease in trabecular volumetric BMD/TV and bone volume fraction BV/TV. Therefore, despite the similar percentage decline of BMD with hind-limb unloading as compared to lactation, no significant differences in lacunar area were observed.

Osteocytes express osteoclast-specific markers during lactation

To identify the molecular mechanisms responsible for removal of mineral by osteocytes, we defined differences in gene expression in osteocytes harvested from virgin, lactating and weaned animals (n=3). Osteocyte-enriched bone was prepared by digesting away the bone surface cells including osteoclasts and osteoblasts. Figure 4a shows 8 genes whose expression was found to be significantly increased during lactation compared to virgin or post-lactation animals (fold >1.5). This list includes genes typically considered osteoclast-specific, such as *TRAP*, *cathepsin K*, *ATP6v0d2*, *ATP6v1g1*, *carbonic anhydrase 1* and *2*, *Nhedc2*, and *MMP13*. Interestingly, there was very low or negligible expression (within baseline noise) of other genes known to be highly expressed in osteoclasts such as *Rank*, *TRAF6*, *calcitonin receptor* or *chloride channel 7*. Furthermore, the expression of *Dentin matrix protein 1*, a marker of early osteocytes, and *Sost*, a marker of late osteocytes was highly elevated (the signal intensities by MAS5 are 2896 for *DMP1*, 5413 for *Sost*, and 13, within baseline, for *Rank*), confirming that samples were highly osteocyte enriched. Together these results confirm a lack of contaminating or infiltrating osteoclasts and suggest that the upregulation of the subset of osteoclast-specific genes shown in Figure 4 occurs specifically in osteocytes.

We chose to focus further studies on TRAP and cathepsin K. In order to validate the microarray data, qPCR was used to analyze the expression of these genes in osteocyte-enriched bones. Consistent with the microarray data, qPCR showed a significant ($p<0.05$) increase of *TRAP* (5.7±3.4 fold) and *cathepsin K* (3.5±0.6 fold) mRNA in osteocytes from lactating mice as compared to virgin and post-lactation animals (Figure 4b,c).

In order to ensure that the changes in *TRAP* were truly specific to osteocytes, we next examined protein expression. It had previously been shown that TRAP, a standard marker of osteoclasts, can be expressed in some osteocytes[24]. As shown in Figure 5a, TRAP activity was significantly elevated in osteocytes in lactating as compared to virgin and post-lactation mice. The induction of TRAP activity correlated with the enlargement of osteocyte lacunae during lactation. In contrast, there were no significant differences in TRAP activity in osteocytes from unloaded as compared to control bones in the hind-limb suspension model correlating with the lack of any increase in osteocyte lacunar size (Figure 5b).

PTHrP treatment simulates trabecular osteocyte perilacunar bone loss and increased TRAP expression similar to lactation

Lactation is associated with elevated circulating parathyroid hormone-related protein (PTHrP) levels[11]. We have previously observed that infusion of PTHrP (1–36) into virgin mice for 11 days caused a modest degree of bone loss both at the spine (5.2±1.2%) and at the femur (4.5±1.8%)[13]. BSEM showed osteocyte lacunar area was significantly increased in vertebral trabecular bone (34.1±2.3*, μm^2) from PTHrP-treated mice as compared to placebo-treated mice (30.7±1.9) *$p<0.05$ (n=5). Though elevated, no significant increase was found in cortical bone. This suggests that trabecular osteocytes respond earlier or more rapidly to 11 days of treatment with PTHrP than do cortical osteocytes. The percentage of TRAP-positive osteocytes was also significantly elevated in PTHrP-treated mice (TRAP+ osteocyte percentage 17.0±4.3% in cortical bone*; 9.4±3.4% in trabecular bone*) as compared to placebo-treated mice (3.4±2.0% cortical; 1.4±0.6% trabecular) (Figure 5c,d). These data indicate that PTHrP is able to stimulate osteocytic perilacunar remodeling and TRAP expression in osteocytes[5].

Targeted deletion of PTH receptor 1 prevents osteocyte specific remodeling during lactation and TRAP expression in osteocytes

PTHrP binds and activates the same receptor (PTHR1) as PTH, and the PTHR1 is expressed on osteocytes[25]. Constitutive activation of the PTHR1 in osteocytes (DMP1-caPTHR1) results in extensive intracortical bone remodeling and increased bone mass[26]. Recently, we have shown that targeted ablation of this receptor in osteocytes results in impaired calcium homeostasis[27]. Therefore, we hypothesized that PTHrP might induce osteocytic perilacunar remodeling by activating the PTHR1 in osteocytes. DMP-Cre/PTHR1$^{lox/lox}$ (PTHR1 cKO) lactating and virgin mice were examined. As shown in Figure 6a, mice lacking the PTHR1 in osteocytes (DMP-Cre PPRfl/fl), did not lose as much bone as the control animals (DMP-Cre/PTHR1$^{lox/+}$; PPR $^{lox/lox}$; PPR $^{lox/+}$) during lactation. In addition, unlike the control mice, which showed significantly enlarged lacunae during lactation, lacunar size did not increase in either trabecular or cortical bone in PTHR1 cKO mice, suggesting that the cKO mice failed to remodel their perilacunar matrix (Figure 6b and c). Consistent with this observation, TRAP activity (Figure 6d,e) did not increase in osteocytes from the cKO mice during lactation. As expected, the number of TRAP-positive osteocytes increased in control animals during lactation (27.4±9.6%) as compared to virgins (0.7%±0.9%).

Cathepsin K is increased in osteocytes during lactation

Immunohistochemical staining demonstrated that cathepsin K was significantly increased in osteocytes during lactation compared to virgin and post-lactation osteocytes (1.33 ± 0.06 virgin, 2.15 ± 0.7* lactating, 1.67 ± 0.7 post-lactation, $p<0.001$, n=3–4 per group) correlating well with gene expression as shown in Figure 4. Simultaneous immunohistochemical staining of wild-type virgin and lactating animals virgin and lactating PTHR1cKO, and the PTHrP injected animals showed significant expression in the lactating wild-type animals, but no significant increases with lactating PTHR1cKO or lactating PTHrP injected animals (Figure 7a,b). Cathepsin K protein tended to be higher in osteocytes from animals injected with PTHrP, but this difference was not statistically different with quantification (Figure 7b). In addition, the expression of lacZ in osteocytes from lactating cathepsin K-Cre/R26R mice was elevated compared to virgin controls (Figure 7c). As shown in Figure 7c middle panel, the *cathepsin K* promoter was active in some osteocytes in virgin mice but many more osteocytes expressed cathepsin K-Cre with greater intensity during lactation (Figure 7c lower panel). As this mouse model is a Cre-knock-in, the endogenous promoter is being utilized providing further evidence of endogenous expression in osteocytes. Together with the immunolocalization staining for protein, these data clearly demonstrate that osteocytes express cathepsin K that is elevated during lactation.

Discussion

As early as 100 years ago, enlarged osteocyte lacunae were noted in human bone[28] and 50 years later it was reported that, in rats treated with parathyroid extract, the unmineralized area around osteocyte lacunae and canaliculi stained positive with periodic acid-Schiff[29]. In the following decades, similar findings were reported in response to PTH treatment, low-calcium diets[30–32], in uremic patients[33], in monkeys subjected to microgravity, and during hibernation[34, 35]. This was referred to as “osteocytic osteolysis” by Belanger[22], but the phenomenon remained controversial and was never generally accepted[36, 37]. In 1977, “osteocytic osteolysis” was suggested to be an artifact of tissue processing and it was argued that osteoclastic activity was sufficient to explain bone resorption[38]. Osteocytic osteolysis was further rebutted when it was reported that, unlike osteoclasts, isolated avian osteocytes did not form resorption lacunae when cultured on sperm whale dentin[39]. As a result, current teaching holds that osteocytes cannot resorb bone. However, utilizing sensitive techniques such as BSEM, quantitative resin casting and dual fluorochrome labeling, the

present studies demonstrate that osteocytes can clearly remove mineral from their surroundings and subsequently replace it in a cyclical fashion. These data demonstrate that reversible osteocytic osteolysis does indeed occur and, furthermore, demonstrate that it is part of the normal adaptation of bone and calcium metabolism to the demands of reproduction.

We found that TRAP mRNA and activity were elevated in osteocytes during lactation. Nakano and co-workers[24] had shown previously that osteocytes can express both TRAP mRNA and protein, but they generally found this within those osteocytes in close proximity to osteoclasts. However, in our studies TRAP-positive osteocytes were also found deep within the bone away from osteoclasts on the bone surface. We found a similar pattern for cathepsin K expression. These enzymes are more active at a low pH and our microarray data demonstrate the osteocytes upregulate genes involved in proton transport during lactation. Therefore, it is likely that osteocytes mimic osteoclasts by reducing the pH within their lacunae and secreting enzymes such as TRAP and cathepsin K in order to remodel the perilacunar matrix. Future studies performing targeted disruption of these genes in osteocytes should determine if they are required for perilacunar remodeling.

Lacunar size returned to normal by 7 days post-lactation. The replacement of mineral during this time is in agreement with studies showing that osteocytes in egg-laying hens have osteoblastic capacity and form new bone around osteocyte lacunae[40]. The double fluorochrome labeling of perilacunar matrix in mice recovering from lactation supports this hypothesis. At this time, it is not known if this process represents a reversible demineralization that preserves matrix or if the matrix is also removed and resynthesized as BSEM only detects mineral and resin can fill in osteoid matrix. Resolving this issue will require future experiments.

Like lactation, mechanical disuse also induces rapid bone loss. We found that in CD1 mice, the extent of bone loss caused by tail suspension was similar to that observed with lactation. Nevertheless, we did not see significant osteocyte perilacunar/canalicular remodeling during unloading, suggesting that osteocytic osteolysis does not accompany rapid bone loss from all causes. A major difference between unloading-induced bone loss and lactation-induced bone loss is that lactation is dominated by changes in hormones, specifically PTHrP, estrogen and prolactin, while it is known that during unloading, circulating levels of PTH and PTHrP are not increased[41]. However, lactation failed to increase osteocyte remodeling in the calvaria, which is an unloaded bone. Thus, this response may also require some input from mechanical coupling.

The demand for calcium during lactation is high and mammals uniformly call on skeletal reserves in order to meet the demands of milk production. It had been previously assumed that osteoclasts were totally responsible for removal of bone for this purpose. Recently it has been shown that targeted deletion of the PTHR1 in osteocytes results in an impaired calcemic response[27], suggesting that osteocytes may also be involved in calcium homeostasis. Our present data suggest that osteocytes contribute to the removal of mineral from the skeleton during lactation by remodeling of their micro-environment; i.e. the perilacunar/canalicular matrix.

PTH has potent anabolic and catabolic effects on bone that differ in response to continuous versus intermittent exposure. Likewise, PTHrP given intermittently increases bone mass, while PTHrP infused continuously or secreted by tumors leads to bone loss. PTHrP targets the same receptor (PTHR1) as PTH, and circulating levels are elevated during lactation and induce bone resorption[11]. The PTHR1 PTHR1 has been identified in osteocytes[25], and expression of a constitutively active PTH1 receptor on osteocytes causes intracortical bone

remodeling[26]. The data in this report suggests that, during lactation, circulating PTHrP interacts with the PTHR1 on osteocytes to induce the expression of a subset of "osteoclast-specific" genes that enable these cells to remove mineral. The importance of PTHrP, signaling through the osteocyte PTHR1, during lactation is demonstrated by the lack of increase in osteocyte lacunae and significantly less bone loss in lactating PTHR1 cKO compared to controls. Consistent with these data, some older reports suggested that osteocytic osteolysis occurred in response to treatment with exogenous PTH. Thus, one might predict that osteocytic perilacunar/canalicular remodeling may contribute to changes in bone during hyperparathyroidism. Our data also raise the interesting possibility that a similar process may contribute to the normal physiological effects of PTH on skeletal calcium mobilization. In this respect, it will be interesting to study whether activation of this pathway requires continuous PTHR1 signaling as occurs during lactation, or whether it can also be activated by intermittent PTHR1 signaling.

In summary, we have found that osteocytes, like osteoclasts, can remove their surrounding mineralized matrix. Under the influence of PTHR1 signaling, osteocytes remove perilacunar mineral with lactation and replace it as the skeleton recovers postweaning. These findings demonstrate that, as with phosphate metabolism, osteocytes contribute directly to the regulation of calcium homeostasis. Furthermore, they demonstrate that certain aspects of the osteoclast phenotype and the ability to mobilize bone mineral can be induced in cells from the mesenchymal/osteoblast lineage in a regulated fashion. These findings have implications for conditions such as hypercalcemia of malignancy and hyperparathyroidism where elevated PTHrP or PTH may cause pathological osteocytic remodeling in contrast to the physiological states of lactation and weaning.

Acknowledgments

We would like to acknowledge Xiaoxiang Ma and Mark Dallas for quantitation of osteocyte lacunae or canalicular width, Carrie Zhao for assistance with the animal husbandry and Kevin J. Barry for technical support. This work was supported by NIH/NIAMS grant PO1 AR046798 (LFB), NIH/NIDDK grant DK079161 (PDP) NIH/NIDDK grant R01 DK073941 (JW), and NIH/NCI grant CA153702 (JW), NIH/NIDDK grant K08 DK081731 (LA). The authors declare that they have no competing financial interests.

References

1. Bonewald LF. The amazing osteocyte. J Bone Miner Res. 2011; 26(2):229–238. [PubMed: 21254230]
2. Poole KE, van Bezooijen RL, Loveridge N, Hamersma H, Papapoulos SE, Lowik CW, Reeve J. Sclerostin is a delayed secreted product of osteocytes that inhibits bone formation. Faseb J. 2005; 19(13):1842–1844. [PubMed: 16123173]
3. Tatsumi S, Ishii K, Amizuka N, Li M, Kobayashi T, Kohno K, Ito M, Takeshita S, Ikeda K. Targeted ablation of osteocytes induces osteoporosis with defective mechanotransduction. Cell Metab. 2007; 5(6):464–475. [PubMed: 17550781]
4. Feng JQ, Ward LM, Liu S, Lu Y, Xie Y, Yuan B, Yu X, Rauch F, Davis SI, Zhang S, Rios H, Drezner MK, Quarles LD, Bonewald LF, White KE. Loss of DMP1 causes rickets and osteomalacia and identifies a role for osteocytes in mineral metabolism. Nature genetics. 2006; 38(11):1310–1315. [PubMed: 17033621]
5. Tazawa K, Hoshi K, Kawamoto S, Tanaka M, Ejiri S, Ozawa H. Osteocytic osteolysis observed in rats to which parathyroid hormone was continuously administered. Journal of bone and mineral metabolism. 2004; 22(6):524–529. [PubMed: 15490261]
6. Marenzana M, Shipley AM, Squitiero P, Kunkel JG, Rubinacci A. Bone as an ion exchange organ: evidence for instantaneous cell-dependent calcium efflux from bone not due to resorption. Bone. 2005; 37(4):545–554. [PubMed: 16046204]
7. Teti A, Zallone A. Do osteocytes contribute to bone mineral homeostasis? Osteocytic osteolysis revisited. Bone. 2009; 44(1):11–16. [PubMed: 18977320]

8. Donahue HJ. Gap junctions and biophysical regulation of bone cell differentiation. Bone. 2000; 26:417–422. [PubMed: 10773579]

9. Kovacs CS, Kronenberg HM. Maternal-fetal calcium and bone metabolism during pregnancy, puerperium, and lactation. Endocrine reviews. 1997; 18(6):832–872. [PubMed: 9408745]

10. Wysolmerski JJ. Interactions between breast, bone, and brain regulate mineral and skeletal metabolism during lactation. Annals of the New York Academy of Sciences. 2010; 1192:161–169. [PubMed: 20392232]

11. VanHouten JN, Wysolmerski JJ. Low estrogen and high parathyroid hormone-related peptide levels contribute to accelerated bone resorption and bone loss in lactating mice. Endocrinology. 2003; 144(12):5521–5529. [PubMed: 14500568]

12. Ardeshirpour L, Dann P, Adams DJ, Nelson T, VanHouten J, Horowitz MC, Wysolmerski JJ. Weaning triggers a decrease in receptor activator of nuclear factor-kappaB ligand expression, widespread osteoclast apoptosis, and rapid recovery of bone mass after lactation in mice. Endocrinology. 2007; 148(8):3875–3886. [PubMed: 17495007]

13. Ardeshirpour L, Brian S, Dann P, VanHouten J, Wysolmerski J. Increased PTHrP and decreased estrogens alter bone turnover but do not reproduce the full effects of lactation on the skeleton. Endocrinology. 2010; 151(12):5591–5601. [PubMed: 21047946]

14. Lu Y, Xie Y, Zhang S, Dusevich V, Bonewald LF, Feng JQ. DMP1-targeted Cre expression in odontoblasts and osteocytes. Journal of dental research. 2007; 86(4):320–325. [PubMed: 17384025]

15. Kobayashi T, Chung UI, Schipani E, Starbuck M, Karsenty G, Katagiri T, Goad DL, Lanske B, Kronenberg HM. PTHrP and Indian hedgehog control differentiation of growth plate chondrocytes at multiple steps. Development (Cambridge, England). 2002; 129(12):2977–2986.

16. Soriano P. Generalized lacZ expression with the ROSA26 Cre reporter strain. Nature genetics. 1999; 21(1):70–71. [PubMed: 9916792]

17. Nakamura T, Imai Y, Matsumoto T, Sato S, Takeuchi K, Igarashi K, Harada Y, Azuma Y, Krust A, Yamamoto Y, Nishina H, Takeda S, Takayanagi H, Metzger D, Kanno J, Takaoka K, Martin TJ, Chambon P, Kato S. Estrogen prevents bone loss via estrogen receptor alpha and induction of Fas ligand in osteoclasts. Cell. 2007; 130(5):811–823. [PubMed: 17803905]

18. Gu G, Nars M, Hentunen TA, Metsikko K, Vaananen HK. Isolated primary osteocytes express functional gap junctions in vitro. Cell Tissue Res. 2006; 323(2):263–271. [PubMed: 16175387]

19. Hens JR, Wilson KM, Dann P, Chen X, Horowitz MC, Wysolmerski JJ. TOPGAL mice show that the canonical Wnt signaling pathway is active during bone development and growth and is activated by mechanical loading in vitro. J Bone Miner Res. 2005; 20(7):1103–1113. [PubMed: 15940363]

20. Lane NE, Yao W, Balooch M, Nalla RK, Balooch G, Habelitz S, Kinney JH, Bonewald LF. Glucocorticoid-treated mice have localized changes in trabecular bone material properties and osteocyte lacunar size that are not observed in placebo-treated or estrogen-deficient mice. J Bone Miner Res. 2006; 21(3):466–476. [PubMed: 16491295]

21. Ardeshirpour L, Dann P, Pollak M, Wysolmerski J, VanHouten J. The calcium-sensing receptor regulates PTHrP production and calcium transport in the lactating mammary gland. Bone. 2006; 38(6):787–793. [PubMed: 16377269]

22. Belanger LF. Osteocytic osteolysis. Calcif Tissue Res. 1969; 4(1):1–12. [PubMed: 4310125]

23. Klein-Nulend J, van der PA, Semeins CM, Ajubi NE, Frangos JA, Nijweide PJ, Burger EH. Sensitivity of osteocytes to biomechanical stress in vitro. FASEB J. 1995; 9(5):441–445. [PubMed: 7896017]

24. Nakano Y, Toyosawa S, Takano Y. Eccentric localization of osteocytes expressing enzymatic activities, protein, and mRNA signals for type 5 tartrate-resistant acid phosphatase (TRAP). J Histochem Cytochem. 2004; 52(11):1475–1482. [PubMed: 15505342]

25. Fermor B, Skerry TM. PTH/PTHrP receptor expression on osteoblasts and osteocytes but not resorbing bone surfaces in growing rats. J Bone Miner Res. 1995; 10(12):1935–1943. [PubMed: 8619374]

26. O'Brien CA, Plotkin LI, Galli C, Goellner JJ, Gortazar AR, Allen MR, Robling AG, Bouxsein M, Schipani E, Turner CH, Jilka RL, Weinstein RS, Manolagas SC, Bellido T. Control of bone mass

and remodeling by PTH receptor signaling in osteocytes. PloS one. 2008; 3(8):e2942. [PubMed: 18698360]

27. Powell WF, Barry KJ, Tulum I, Kobayashi T, Harris SE, Bringhurst F, Divieti Pajevic P. Targeted ablation of the PTH/PTHrP receptor in osteocytes impairs bone structure and homeostatic calcemic responses. The Journal of endocrinology.
28. von Recklinghausen, FV. Untersuchungen uber Rachitis und Osteomalacia. Jena: Gustav Fischer; 1910.
29. Heller-Steinberg M. Ground substance, bone salts, and cellular activity in bone formation and destruction. Am J Anat. 1951; 89(3):347–379. [PubMed: 14894444]
30. Baud, CA.; Dupont, DH. Electron Microscopy. SS Breese, J., editor. Vol. 2. Academic Press; New York: 1962. p. QQ-10.
31. Belanger LF, Drouin P. Osteolysis in the frog. The effects of parathormone. Canadian journal of physiology and pharmacology. 1966; 44(6):919–922. [PubMed: 5970233]
32. Belanger LF, Jarry L, Uhthoff HK. Osteocytic osteolysis in Paget's disease. Revue canadienne de biologie / editee par l'Universite de Montreal. 1968; 27(1):37–44.
33. Bonucci E, Gherardi G. Osteocyte ultrastructure in renal osteodystrophy. Virchows Arch A Pathol Anat Histol. 1977; 373(3):213–231. [PubMed: 140505]
34. Iagodovskii VS, Triftanidi LA, Gorokhova GP. Effect of space flight on rat skeletal bones (an optical light and electron microscopic study). Kosmicheskaia biologiia i aviakosmicheskaia meditsina. 1977; 11(1):14–20. [PubMed: 839704]
35. Haller AC, Zimny ML. Effects of hibernation on interradicular alveolar bone. Journal of dental research. 1977; 56(12):1552–1557. [PubMed: 277478]
36. Gay CV, Mueller WJ. Carbonic anhydrase and osteoclasts: localization by labeled inhibitor autoradiography. Science (New York, NY). 1974; 183(123):432–434.
37. Rasmussen P. Calcium deficiency, pregnancy, and lactation in rats. Microscopic and microradiographic observations on bones. Calcif Tissue Res. 1977; 23(1):95–102. [PubMed: 890546]
38. Parfitt AM. The cellular basis of bone turnover and bone loss: a rebuttal of the osteocytic resorption–bone flow theory. Clin Orthop Relat Res. 1977; (127):236–247. [PubMed: 912987]
39. van der Plas A, Aarden EM, Feijen JH, de Boer AH, Wiltink A, Alblas MJ, de Leij L, Nijweide PJ. Characteristics and properties of osteocytes in culture. J Bone Miner Res. 1994; 9(11):1697–1704. [PubMed: 7863820]
40. Zambonin Zallone A, Teti A, Primavera MV, Pace G. Mature osteocytes behaviour in a repletion period: the occurrence of osteoplastic activity. Basic and applied histochemistry. 1983; 27(3):191–204. [PubMed: 6196018]
41. Sarli M, Hakim C, Rey P, Zanchetta J. Osteoporosis during pregnancy and lactation. Medicina. 2005; 65(6):533–540. [PubMed: 16433484]

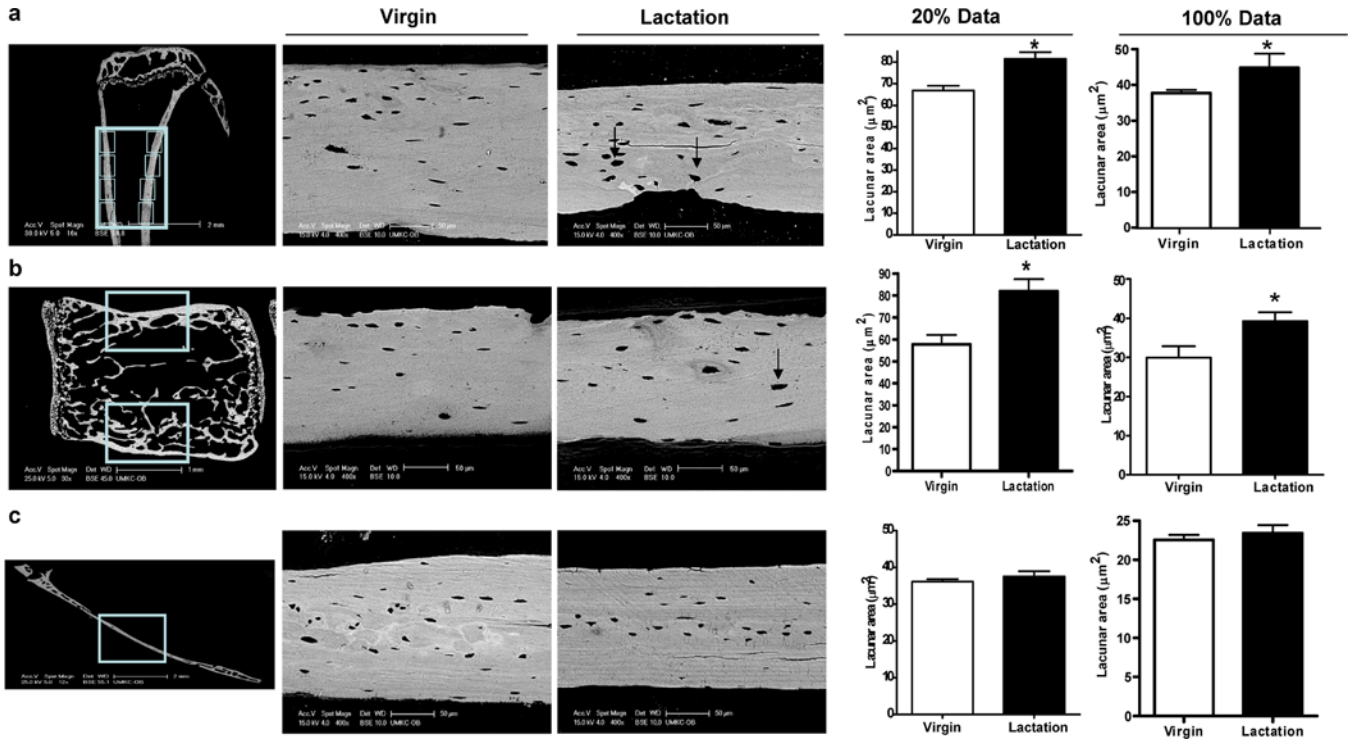

Figure 1.

Osteocyte lacunar area increases in tibiae and lumbar vertebrae, but not in parietal calvarial bone during lactation. (*A*) Eight BSEM images (locations are shown by boxes) were taken on the cortical bone of each tibia from virgin and lactating mice and osteocyte lacunar size was quantified. A significant increase was observed in lactating animals regardless of whether the largest 20% of lacunae were compared or 100% of lacunae. (*B*) BSEM images (box) were taken on the cortical bone of LV1–LV4 from virgin and lactating mice. A significant increase in osteocyte lacunar area (in m^2) was observed using 20% of the largest lacunae during lactation as compared to virgin mice (*$p < 0.05$; $n = 3$). Lacunar area was also increased using 100% of the lacunae but the difference did not reach significance. BSE images showed that during lactation osteocyte lacunae enlarged with irregular borders (black arrow). (*C*) Sagittal sections were made 2 mm right of the middle sagittal suture in the right parietal bone. BSEM were used to image osteocyte lacunae in the middle of sagittal parietal bone (box). BSEM images of parietal bone show no obvious remodeled osteocyte lacunae. Quantitation of the BSEM images showed no significant change in osteocyte lacunar area from parietal bone during lactation compared to virgin mice ($n = 8$).

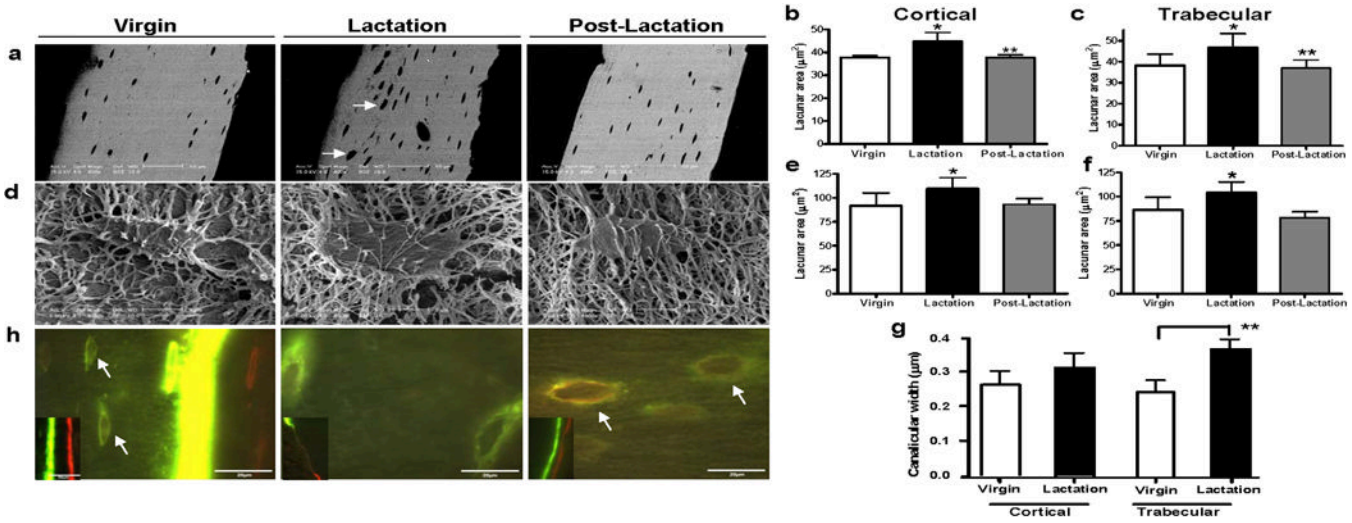

Figure 2.

Lactation induces osteocytic remodeling during lactation that returns to virgin levels with postlactation. (*A*) BSEM showed that during lactation osteocyte lacunae enlarged with irregular borders indicating mineral removal (white arrows). (*B*) Osteocyte lacunar area (in μm^2) was significantly increased in cortical bone during lactation as compared to virgin or 7 days postlactation. (Experiment repeated four times; $*p < 0.05$; $**p < 0.01$; $n = 7–9$ per group). (*C*) Osteocyte lacunar area (in μm^2) was significantly increased in trabecular bone during lactation as compared to virgin or 7 days postlactation ($*p < 0.05$; $**p < 0.01$; $n = 7–9$ per group). (*D*) Osteocyte lacunae were imaged using acid-etch resin-casted SEM to further validate the measurements by SEM. (*E*) Osteocyte lacunar area measured by acid-etch resin-casted SEM was significantly increased in cortical bone during lactation as compared to virgin or 7 days postlactation ($*p < 0.05$; $n = 4–5$ per group). (*F*) Osteocyte lacunar area measured by acid-etch resin-casted SEM was significantly increased in trabecular bone during lactation as compared to virgin or 7 days postlactation ($*p < 0.05$; $n = 4–5$ per group). (*G*) The same resin-casted SEM images were also used to measure canalicular diameter. An increase in canalicular diameter was observed in cortical bone from lactating animals and a significant increase in trabecular bone ($p < 0.001$; $n = 4–5$ per group). (*H*) Double fluorochrome labeling. Two distinctive lines of fluorochrome labeling, calcein green (first injection) and Alizarin red (second injection), can be found at the bone surface (smaller image insert). In the virgin animal, faint label was taken up by the newly embedding osteocytes at the mineralization front (arrows in virgin). Only green labeling was observed in the lactating animals and an intermittent green label on the bone surface. Lacunae labeled with both fluorochromes (mixed green and red bands) were observed distant from the mineralization front (previously existing lacunae) in the postlactation animals (white arrows in postlactation).

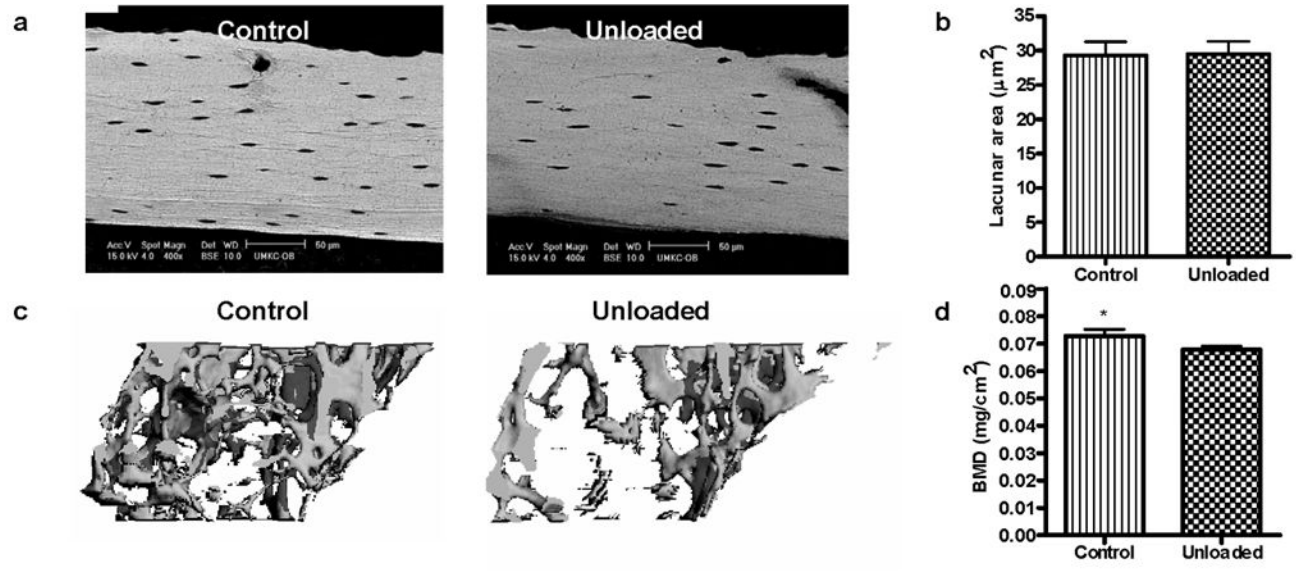

e Results of quanitative microCT analysis of left proximal tibiae

	Cortical and trabecular bone		Trabecular bone				
	BMD/TV(mg/ccmHA)	BV/TV(%)	BMD/TV(mg/ccmHA)	BV/TV(%)	TB.N(1/mm)	TB.TH(μm)	TB.Sp
Control(n=7)	341.70±38.37	0.40±0.02	84.44±25.67	0.12±0.02	2.45±0.43	0.06±0.004	0.38±0.17
Unloading(n=6)	268.37±40.18	0.32±0.03	52.50±16.42	0.07±0.02	1.92±0.20	0.05±0.004	0.54±0.05
P values	0.006	<0.001	0.024	<0.001	0.018	0.009	0.062

Figure 3.

Mechanical disuse does not induce osteocytic remodeling. (*A*) BSE imaging of osteocyte lacunae. (*B*) Osteocyte lacunar size was measured using backscatter SEM in the same procedures as for the lactating mouse. Even though the age-matched unloaded CD1 female mice lost BMD/TV and BV/TV (by μCT), backscatter SEM showed that the osteocyte lacunar area did not significantly change ($p = 0.87$; $n = 7$ per group) in cortical bone in hindlimb-unloaded mice compared to controls. Lack of significant differences was also observed in trabecular bone (data not shown). (*C*) Unloaded trabecular bone architecture by μCT showed bone loss during unloading compared to control. BMD was significantly decreased ($p < 0.0001$; 7.4% bone loss) in the left femur of unloaded mice compared to controls. (*D*) BMD (mg/cm^2) significantly decreased ($p = 0.01$) in femur during unloading compared to ambulatory controls. A similar effect was seen in the proximal tibiae (data not shown) (*$p < 0.05$; $n = 7$ per group). (*E*) Table of μCT analyses. BMD = bone mineral density; BV = bone volume; TV = total volume; TB.N = trabecular number; TB.TH = trabecular bone thickness; TB.Sp = trabecular bone space.

a

Gene name	Signal intensity (average of 3 arrays)			Fold change	
	Virgin	Lactation	Post Lactation	Lactation /Virgin	Post Lactaticn /Lactation
tartrate resistant acid phosphatase 5, TRAP	1824 +/- 229	6075 +/- 832	1919 +/- 562	3.3**	– 3.4*
Cathepsin K, Ctsk	1269 +/- 213	4530 +/- 562	1845 +/- 379	3.6**	– 2.5**
carbonic anhydrase 2, Car2	2613 +/- 549	4681 +/- 543	369 +/- 42	1.8*	– 12.7**
carbonic anhydrase 1, Car1	921 +/- 247	1924 +/- 274	91 +/- 19	2.2*	– 9.8**
Na+/H+ exchanger domain containing 2, Nhedc2	105 +/- 13	356 +/- 41	126 +/- 35	3.4**	– 3.0**
ATPase, H+ transporting, lysosomal V1 subunit G1, ATP6V1G1	861 +/- 19	1525 +/- 13	1097 +/- 16	1.8*	– 1.4*
ATPase, H+ transporting, lysosomal V0 subunit D2, ATP6V0D2	149 +/- 4	488 +/- 68	191 +/- 41	3.6**	– 2.9**
matrix metallopeptidase 13, MMP13	3467 +/- 248	6380 +/- 447	2674 +/- 725	1.8**	– 2.4*

[*p<0.05, **P<0.01]

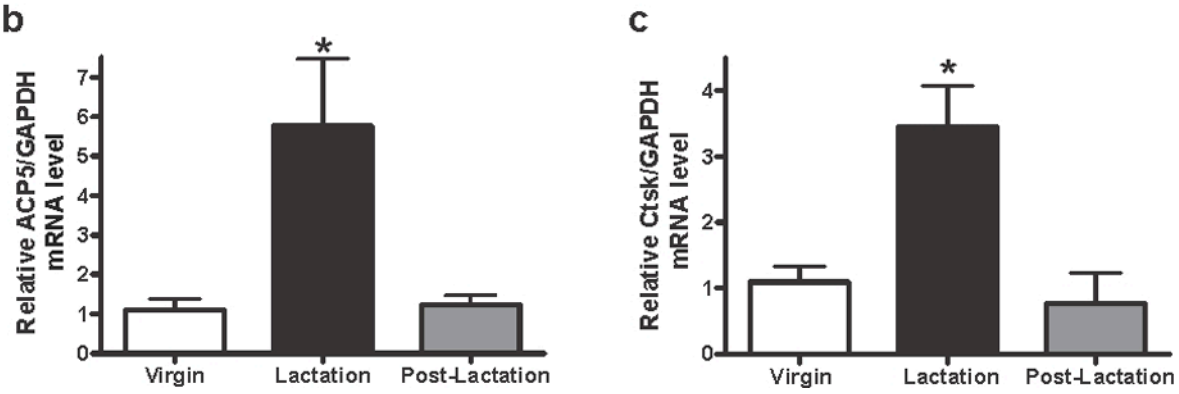

Figure 4.

Expression of several osteoclast-specific genes is increased in osteocytes during lactation. (*A*) Table of microarray data showing significantly changed genes between virgin and lactating animals and between lactating and postlactation animals (*$p < 0.05$; **$p < 0.01$; $n = 3$ per group). (*B*) Using qPCR, ACP5 (TRAP) mRNA level from isolated osteocytes relative to GAPDH was significantly increased during lactation compared to virgin control or postlactation (*$p < 0.05$; $n = 4$ per group). (*C*) Ctsk (cathepsin K) mRNA level from isolated osteocytes relative to GAPDH was significantly higher during lactation than virgin control or postlactation (*$p < 0.05$; $n = 4$ per group).

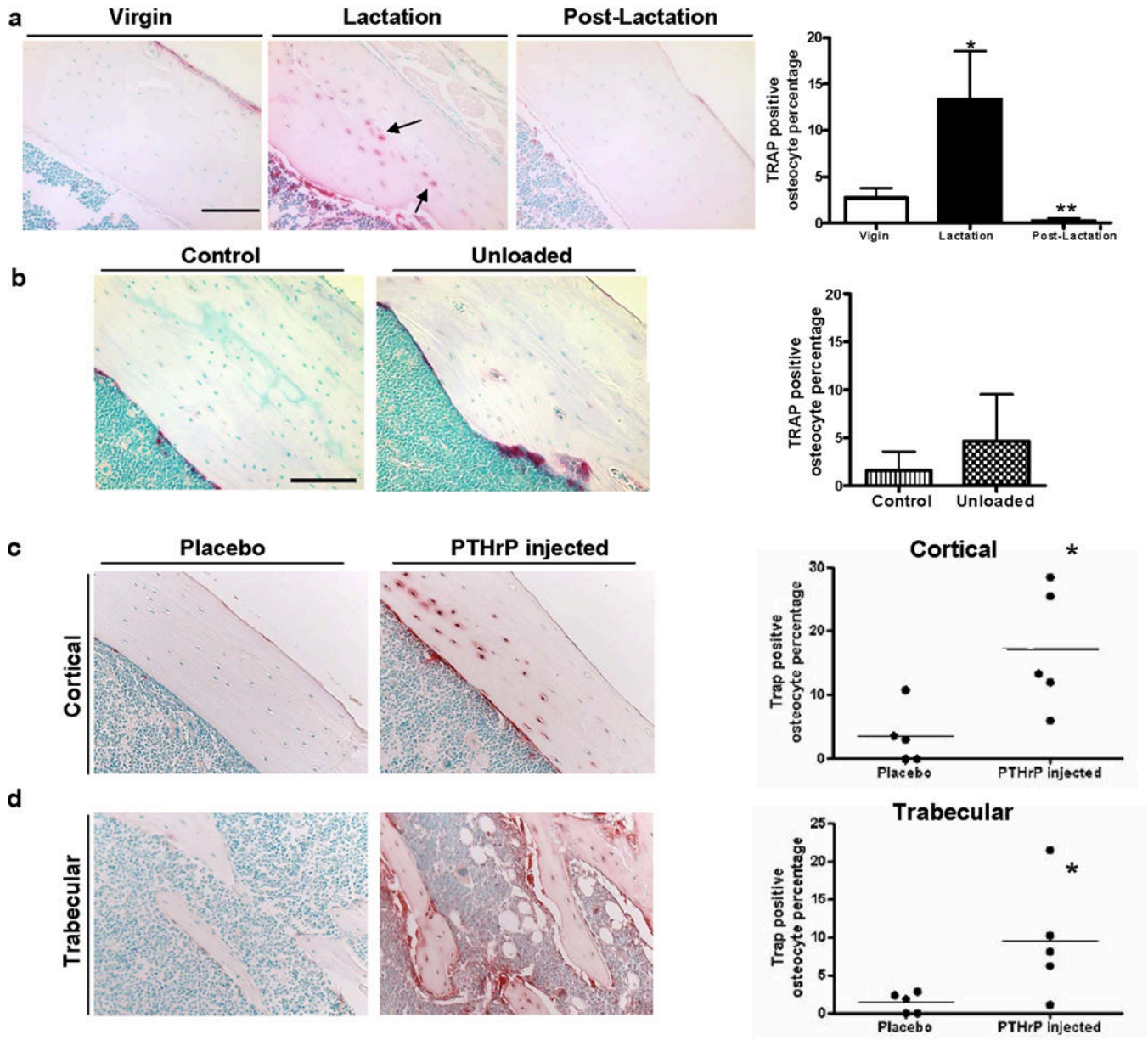

Figure 5.

TRAP is increased during lactation compared to virgin or postlactation animals. No significant changes were observed with unloading. Infusion of PTHrP induces elevation of TRAP in osteocytes. (*A*) TRAP staining showed more TRAP-positive osteocytes during lactation (black arrows). (The periosteal surface is upper right and endocortical surface is lower left.) The percentage of osteocytes with TRAP activity from the lactating mice (13.4% ± 5.2%* TRAP+ osteocytes) was significantly increased compared to the virgin (2.7% ± 1.8%) and day 7 postlactation (0.3% ± 0.5%**) animals (*$p < 0.05$; **$p < 0.01$; $n = 4–5$). (*B*) Tartrate resistant acid phosphatase staining of tibia from control and unloaded animals. No significant difference ($p = 0.28$; $n = 7$ per group) in percent of TRAP-positive osteocytes was observed between control (1.6% ± 1.0%) and unloaded groups (4.6% ± 2.2%). (*C*) Cortical (the periosteal surface is upper right and endocortical surface is lower left.) and (*D*) trabecular bone was stained for TRAP. TRAP staining showed TRAP activity was

significantly elevated in osteocytes in PTHrP-treated mice (TRAP+ osteocytes percentage 17.0% ± 4.3% in cortical bone*; 9.4% ± 3.4% in trabecular bone*) as compared to placebo-treated mice (3.4% ± 2.0% cortical; 1.4% ± 0.6% trabecular) (*$p < 0.05$; $n = 5$).

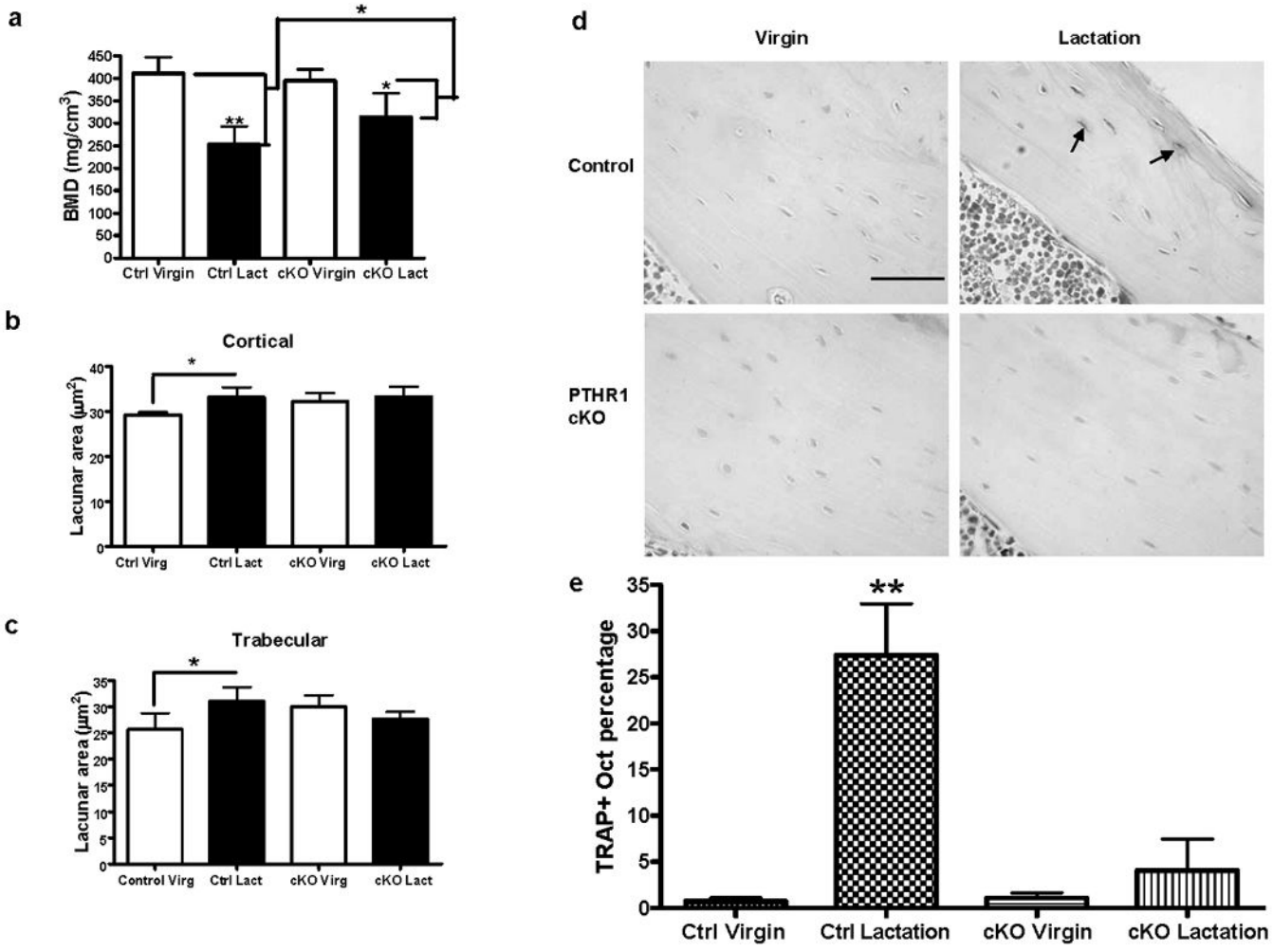

Figure 6.

Osteocyte remodeling during lactation was blocked in osteocyte-specific PTHR1-cKO mice. (*A*) BMD measurement by μCT showed a decrease in bone density in both the control and the PTHR1-cKO mice during lactation. There is less bone density loss (47% attenuation) during lactation in PTHR1-cKO mice (*$p < 0.05$; **$p < 0.01$; $n = 3–6$ per group). (*B*) In control mice, osteocyte lacunar area in tibial cortical bone significantly increased during lactation compared to virgin, while lacunar area did not enlarge in the PTHR1 cKO mice with lactation (*$p < 0.05$; $n = 3–6$ per group). (*C*) In control mice, osteocyte lacunar area in tibial trabecular bone significantly increased during lactation compared to virgin, while lacunar area did not enlarge in the PTHR1 cKO mice with lactation (*$p < 0.05$; $n = 3–6$ per group). (*D*) Tartrate resistant acid phosphatase staining. A significant increase in TRAP-positive osteocytes in control mice with lactation was not observed in the PTHR1-cKO mice. (The periosteal surface is upper right and endocortical surface is lower left.) (*E*) In control mice, a significantly increased number of osteocytes with TRAP activity ($p < 0.01$) in the lactating mice (27.4% ± 9.6%** TRAP+ osteocytes) was observed compared to the virgin mice (0.7% ± 0.9%). There was no significant difference in TRAP activity from PTHR1-cKO mice during lactation (4.1% ± 8.4%) compared to virgin mice (1.1% ± 1.2%) (*$p < 0.05$; **$p < 0.01$; $n = 3–6$ per group).

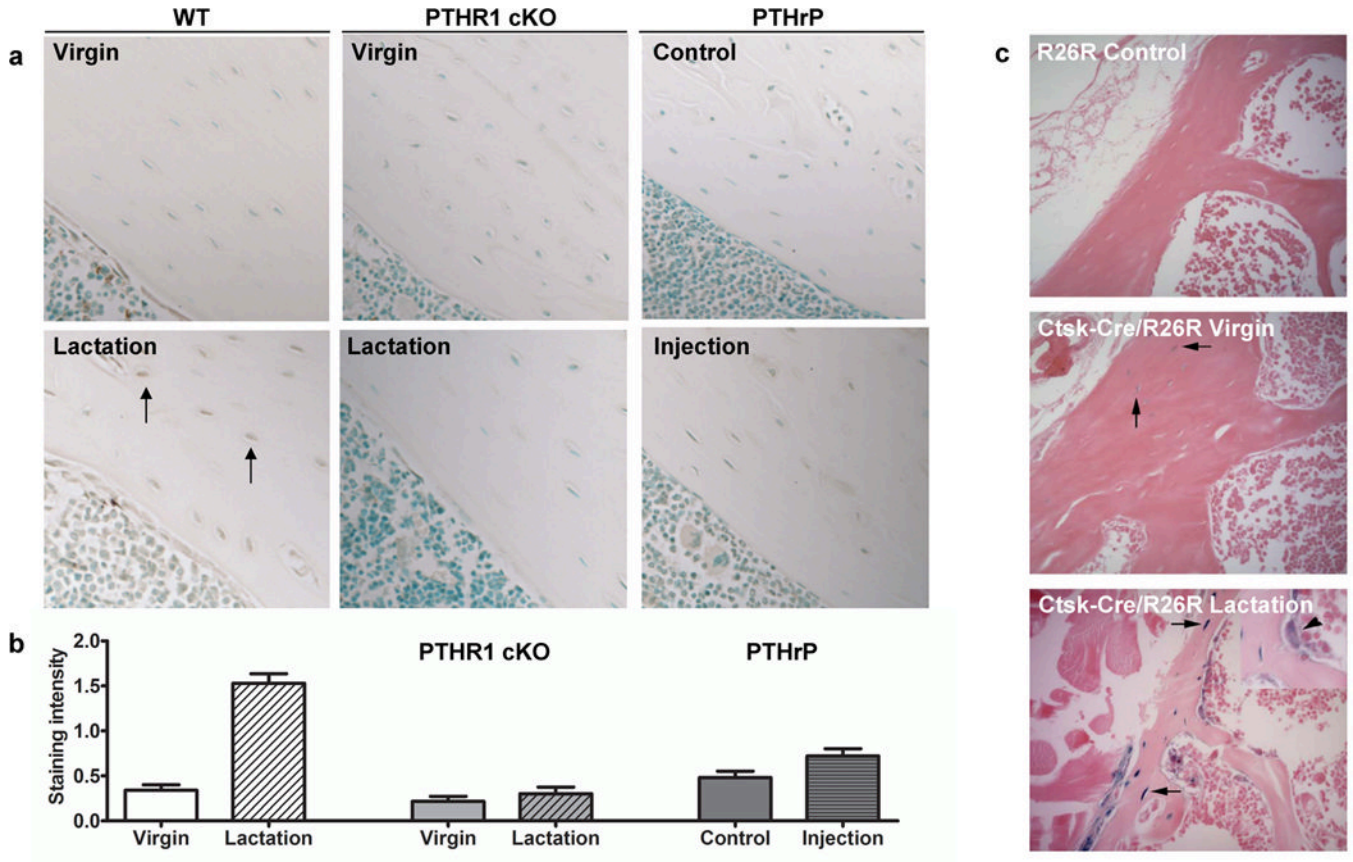

Figure 7.

Cathepsin K protein and gene expression is elevated in osteocytes during lactation. (*A*) Immunostaining for cathepsin K in osteocytes (black arrows), scale bar 100 μM. Increased staining is observed in bone from wild-type lactating animals compared to virgin animals. No obvious increases were observed in PTHR1 cKO virgin or lactating animals, nor significant differences with PTHrP-injected animals compared to vehicle control–injected animals. (*B*) Immunostaining was quantitated on all groups within the same experiment showing significant increases in lactating wild-type animals compared to the other groups. (*C*) Bone from virgin mice containing both the Ctsk-cre and the R26R showed some pale blue staining in osteocytes (arrows, middle panel), whereas bone from lactating animals showed that not only osteoclasts, but more osteocytes express LacZ and thus cathepsin K. The arrowhead (inset, lower panel) indicates the osteoclast as a positive control for beta-galactosidase staining. The R26R control bone (upper panel) shows no blue color, as expected.